Radiative lifetimes of the alkaline earth monohalides

Paul J. Dagdigian, Howard W. Cruse, and Richard N. Zare

Citation: The Journal of Chemical Physics **60**, 2330 (1974); doi: 10.1063/1.1681366
View online: https://doi.org/10.1063/1.1681366
View Table of Contents: http://aip.scitation.org/toc/jcp/60/6
Published by the American Institute of Physics

Radiative lifetimes of the alkaline earth monohalides

Paul J. Dagdigian, Howard W. Cruse*, and Richard N. Zare

Department of Chemistry, Columbia University, New York, New York 10027
(Received 15 November 1973)

The radiative lifetimes for a number of electronic states of the alkaline earth monohalide molecules MX, where M denotes Ca, Sr, or Ba and where X denotes F, Cl, Br, or I, have been determined directly from the rate of fluorescence decay with time using a pulsed dye laser as an excitation source. The measured lifetimes in nanoseconds are CaF: A_1 21.9(4.0), A_2 18.4(4.1), B 25.1(4.0); CaCl: A_1 29.4(1.8), A_2 28.4(2.6), B 38.2(3.9), C 25.0(2.1); CaBr: A_1 34.2(2.9), A_2 33.7(1.9), B 42.9(3.1), C_1 33.2(4.0), C_2 31.8(3.7); CaI: A_1 41.7(2.3), A_2 41.6(3.4), B 50.9(1.7); SrF: A_1 24.1(2.0), A_2 22.6(4.7); SrCl, A_1 31.3(2.7), A_2 30.4(3.6), B 38.8(2.1), C_1 26.1(1.9), C_2 26.0(1.6); SrBr: A_1 34.3(2.3), A_2 33.2(1.6), B 42.2(1.6), C_1 30.3(2.6), C_2 28.1(1.3); SrI: A_1 43.3(1.6), A_2 41.9(1.3), B 46.0(2.0), C_1 36.0(3.7); BaF: C_1 23.8(2.3), C_2 23.5(0.7); BaCl: C_1 17.5(0.8), C_2 16.6(0.6); BaBr: C_1 17.9(1.0), C_2 16.5(1.4); BaI: C_1 17.9(1.9), C_2 16.0(1.5), where A_1, A_2, B, C_1, and C_2 denote, respectively, the $A\ ^2\Pi_{1/2}$, $A\ ^2\Pi_{3/2}$, $B\ ^2\Sigma^+$, $C\ ^2\Pi_{1/2}$, and $C\ ^2\Pi_{3/2}$ states, and where the uncertainties, representing one standard deviation, are given in parentheses. The lifetimes of the CaX and SrX states are seen to be quantitatively similar, while those of BaX are quite different. No vibrational dependence of the lifetime for the BaI C_2 state is observed for $0 \leq v' \leq 39$. For other MX molecules the vibrational dependence of the lifetime could not be ascertained because the MX molecule was not produced in a sufficiently wide range of ground state vibrational levels. Various one-electron models for the MX transitions are discussed. It is found that a consistent explanation of the transition moments can be obtained by assuming that the transition is between two nonbonding orbitals centered on the metal atom whose mixing coefficients in terms of a truncated metal atom basis set are adjusted to reproduce a subset of the experimentally determined transiton moments. For the X, A, and B states of CaX and SrX, the nonbonding orbital is primarily $n\,s\,\sigma$, $n\,p\,\pi$, and $n\,p\,\sigma$, respectively, in character; for BaX it is suggested that $(n-1)d\,\pi$ and $(n-1)d\,\sigma$ play an important role in the description of the nonbonding orbital in the A, B, and C states.

I. INTRODUCTION

The alkaline earth monohalides are an interesting class of molecules having nine valence electrons outside closed shells. The excited states have the remarkable feature that their equilibrium internuclear separations and vibrational frequencies are nearly the same as those of the ground state. Consequently the electronic spectra are characterized by strong and closely spaced $\Delta v = 0$ (diagonal) sequences.[1] Figure 1 gives an energy level diagram of the lowest-lying electronic states of the calcium, strontium, and barium monohalides, hereafter denoted as MX. The relative positions of the energy levels are similar for all three metals and do not depend strongly on the identity of the halogen atom, although there is a weak monotonic trend in going from F to I. It appears that the electronic spectra are characterized by the promotion of a nonbonding electron in a molecular orbital centered primarily on the metal atom to an excited nonbonding orbital also centered on the metal atom. According to this model, the radiative lifetimes of these molecules should be closely related to the metal atom transition moments. In order to investigate this model and, hopefully, to gain insight into the nature of the bonding of the alkaline earth monohalides, a comprehensive study of the radiative lifetimes of the low-lying electronic states of the MX molecules has been undertaken.

II. EXPERIMENTAL

A. Apparatus

The apparatus used to determine radiative lifetimes of the Group IIa monohalides is essentially the same as that employed to measure internal state distributions in products of chemical reactions.[2] Basically it consists of three parts: (1) a reaction chamber to produce ground state MX molecules by an elementary gas-phase chemical reaction between a beam of metal atoms and a suitable halogen containing molecule, (2) a pulsed tunable dye laser to pump MX to an excited electronic state, and (3) a fast photomultiplier and oscilloscope to monitor fluorescence decay from the excited state.

The Ca, Sr, or Ba atomic beam is produced by effusion from a molybdenum oven heated to temperatures between 900 and 1050 °K. The oven is situated in its own separately pumped chamber, and the metal beam passes into the reaction chamber through a slit, 0.2 $\times$ 1.9 cm in size. The reaction chamber consists of a stainless steel tube (70 cm long and 25 cm diam) and is evacuated by two 4-in. diffusion pumps. During the experiments the reaction chamber is filled with reagent gas at pressures between 10^{-5} and 10^{-3} torr (uncorrected ionization gauge readings). It is estimated that the MX molecules are formed in concentrations on the order of 10^8–10^9 molecules cm^{-3}.

The tunable dye laser is pumped by a pulsed nitrogen laser (Avco Everett Research Laboratories Model C950), and the resulting dye laser pulses have an energy of about 10^{-5} J. The laser pulse measured using a fast photodiode (risetime 0.5 nsec) has a fwhm of 3–5 nsec and width of approximately 6–10 nsec at 5% of peak intensity (see Fig. 2). Both energy and pulse width vary with the dye used. It is important to note that there is no detectable "tail" to the laser pulse 15 nsec after the pulse. The small oscillations after the pulse, shown in

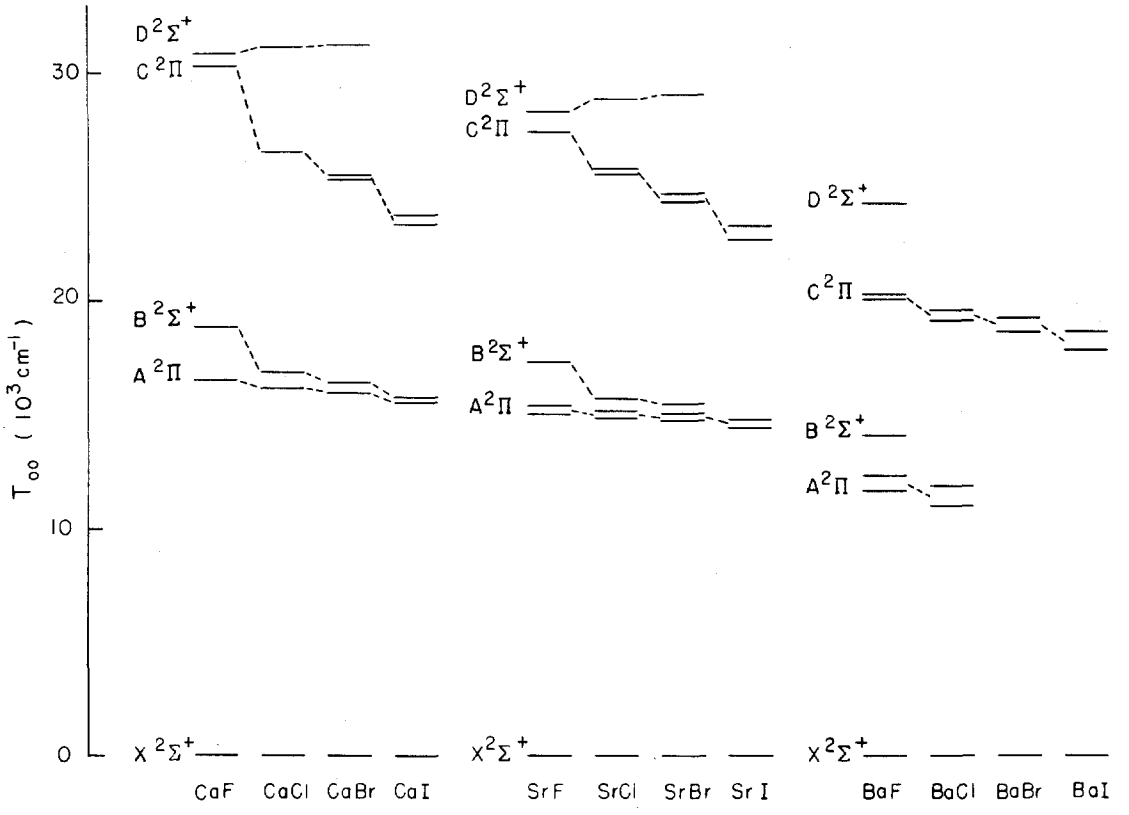

FIG. 1. Observed term values for the lowest-lying electronic states of the calcium, strontium, and barium monohalides. The spin–orbit splitting of some $^2\Pi$ states is too small to be shown.

Fig. 2, are electrical ringing. The dye laser is tunable over the wavelength range 3750–6900 Å using a series of 12 dyes or dye mixtures, [3] and the bandwidth is typically 0.5 Å. During lifetime measurements the dye laser is set to a wavelength that coincides with an electronic absorption band system of MX, and the laser wavelength is determined using a 1-m monochromator. Because of the wavelength range of the dye laser, it is not possible to study the *A* and *B* states of BaX, which lie to the red of 7000 Å. Although the *D* states of BaX can be excited by the dye laser, the weakness of these fluorescence signals prevented accurate lifetime determinations.

Fluorescence from excited MX is detected by an RCA 7265 photomultiplier (S-20 photocathode) and a 7904 Tektronix oscilloscope having a 7B92 time base and a 7A19 amplifier (500 MHz bandwidth). The oscilloscope time base has been calibrated to better than 1% using a signal generator and digital counter. No wavelength selection of the fluorescence is normally employed. However, Corning filters were placed in front of the photomultiplier to study the electronic branching of the fluorescence. Unwanted scattered laser light is rejected by a system of baffles as described in Ref. 2. In the present experiments the scattered light signal is usually less than 1% of the fluorescence signal. The variation of fluorescence intensity during and after a single laser pulse is recorded by photographing the oscilloscope trace.

The fluorescence intensity of a single scan is read off the photograph at equally spaced time intervals. A least squares computer program is then used to analyze these measurements to yield a lifetime. The lifetime of a state is computed as the average of the lifetimes from a number of such scans. Radiative lifetimes are determined from analysis of the portion of the trace 20 nsec or more after the peak fluorescence intensity. (In this time region we can be certain that no laser excitation of MX molecules is taking place.)

B. Production of MX molecules

The reactions used to produce the alkaline earth monohalide molecules are listed in Table I. These re-

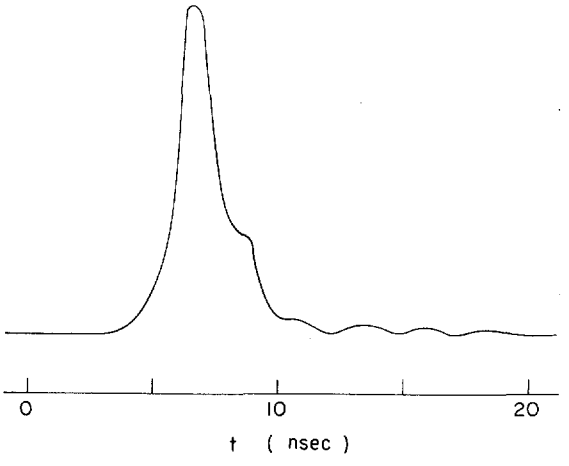

FIG. 2. Typical oscilloscope trace of the dye laser pulse, as detected by a fast photodiode.

TABLE I. Reactions used to produce the calcium, strontium, and barium monohalides.

Reaction	Values of v'' observed	Most populated v'' [a]
$Ca + SF_6 \Rightarrow CaF$ [b]	Not scanned	
$Ca + HCl \rightarrow CaCl + H$	0–2	0
$Ca + HBr \rightarrow CaBr + H$	0–3	0
$Ca + CH_3I \rightarrow CaI + CH_3$	Unresolved	
$Sr + SF_6 \Rightarrow SrF$ [b]	0–3	0
$Sr + HCl \rightarrow SrCl + H$	0–4	1
$Sr + HBr \rightarrow SrBr + H$	0–6	2
$Sr + CH_3I \rightarrow SrI + CH_3$	4–13	10
$Ba + SF_6 \rightarrow BaF + SF_5$	0–6 [c]	0
$Ba + HCl \rightarrow BaCl + H$	0–11 [d]	3
$Ba + HBr \rightarrow BaBr + H$	0–20 [d]	9
$Ba + CH_3I \rightarrow BaI + CH_3$	0–35 [e]	20
$Ba + CH_2I_2 \rightarrow BaI + CH_2I$	25–50 [e]	40

[a] Approximate value.
[b] "Oven reaction" (see text).
[c] Reference 4(b).
[d] Reference 2.
[e] Reference 4(a).

actions are chosen because only ground state molecules are formed. Reactions producing electronically excited products have been avoided because the resulting chemiluminescence hampers detection of the laser-induced fluorescence signal. The MX products are identified by comparing the excitation spectra with known spectroscopic information.[1]

In the present experiments it is possible to obtain information on the collisionally undegraded vibrational distribution of the MX products. For the BaX reactions this information is summarized in Table I and described in detail elsewhere.[2,4] For the CaX and SrX reactions only a crude indication of the vibrational distribution is obtained (see Table I) since the excitation spectra were poorly resolved.

It is simple to produce most of the MX molecules in concentrations suitable for lifetime measurements using gas-phase reactions. However, the production of CaF and SrF presented a problem. It was found that Ca and Sr do not react appreciably with SF_6 in the gas phase, but small amounts of CaF and SrF were formed by an "oven reaction" involving the leakage of small amounts of SF_6 into the oven chamber. These "oven reactions" are characterized by: (1) the independence of the MX fluorescence intensity with SF_6 pressure once the process has been initiated,[5] (2) signal intensities roughly an order of magnitude lower than those resulting from gas-phase reactions, and (3) a thermal vibrational distribution with a temperature equal to that of the oven.

C. Possible systematic errors

Although the method we have used to determine radiative lifetimes is direct, a considerable number of systematic errors could seriously affect the reliability of the results. Here we consider possible sources of systematic error and assess their effect on our data.

1. Electronic quenching

When the collisional rate is comparable to the rate of radiative decay, the effective lifetime may be shortened through quenching. In the present experiments the short lifetimes of the MX molecules, combined with the low gas pressures used, ensure that measurements are taken under collision-free conditions. For example, at the highest pressures used, the quenching rate is calculated to be four orders of magnitude smaller than the rate of radiative decay, assuming a quenching cross section of 10 Å^2.

2. Radiation trapping

When the density of absorbing molecules becomes high enough, it is found that the fluorescence can be trapped by multiple scattering of resonance photons. The trapping of resonance radiation causes an increase in the effective lifetime of excited molecules, which is proportional to the probability that a photon will be absorbed before leaving the vapor. In this experiment the lifetime is expected to be affected negligibly by radiation trapping because of the low density of MX molecules (10^8–10^9 molecules cm^{-3}).

A crude experimental check of radiation trapping and electronic quenching has been made by measuring the lifetime of the $B\,^2\Sigma^+$ state of SrBr at different reactant gas pressures. Raising the reactant gas pressure not only increases the total pressure but also increases the SrBr partial pressure. It is found that the lifetime is the same to within experimental error at two different pressures of HBr (42.2 ± 1.6 nsec at 1.5×10^{-4} torr and 41.5 ± 3.7 nsec at 0.4×10^{-4} torr).

3. Detector response time

The radiative lifetimes reported in this paper lie in the range 15–50 nsec. We have investigated whether our detection system could faithfully reproduce fast signals such as rapid fluorescence decay. First, single photoelectron pulses were observed. They were found to have a risetime (10%–90% of peak intensity) of less than 3 nsec and a fwhm of about 4 nsec. It is calculated that the convolution of a Gaussian pulse (fwhm = 4 nsec) with an exponentially decaying signal ($\tau = 10$ nsec) has a lifetime equal to 10 nsec to an accuracy better than our experimental error, provided that times 5 nsec or more past the peak are used. This implies that our lifetime measurements are not distorted by the finite response time of the detection system. As an experimental check, the lifetime of the Ba $6s6p\,^1P_1$ state was measured with greatly reduced Ba flux to eliminate radiation trapping. We find the lifetime to be 9.1 ± 0.8 nsec, in agreement with the literature values, 8.20 ± 0.20,[6] 8.36 ± 0.25,[7] and 10.4 ± 0.5 nsec.[8] Since the MX lifetimes are all greater than 15 nsec, it is expected that the detector response time will increase the lifetimes by less than 1 nsec.

4. Cascading

It is important to know that the observed fluorescence decay is associated with the decay of only one electronic

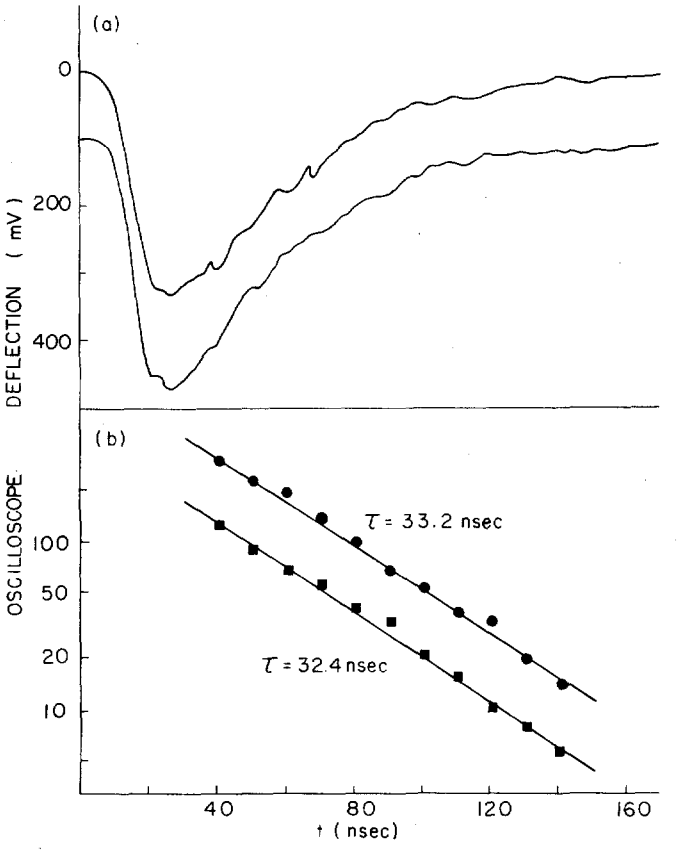

FIG. 3. Typical fluorescence decay curves: The $A\ ^2\Pi_{1/2}$ state of SrBr. (a) Oscilloscope traces. The lower trace is displaced 100 mV. (b) Semilogarithmic plots for the traces in (a). The circles and squares correspond to the upper and lower traces, respectively. The lower trace has been displaced vertically for clarity by multiplying the oscilloscope deflections by a factor of 0.4. The lifetimes determined from the plots are marked.

state. In the past, many lifetime studies have encountered difficulties from cascading processes in which higher states decay to the state under study, causing a lengthening in the measured lifetime. Because the present studies employ resonance fluorescence, this form of cascading has been avoided. However, another type of cascading may occur if the state under study can branch to an intermediate excited state and if the fluorescence from the intermediate state can be detected. Once again the effect of this type of cascading is to lengthen the measured lifetime.

For the A state of the MX molecules, of course, this effect is not present. In the B state there is a possibility of $B \rightarrow A$ branching followed by $A \rightarrow X$ decay. However, the branching ratio of $B \rightarrow A$ to $B \rightarrow X$ decay is expected to be roughly proportional to the cube of the ratio of the transition frequencies and hence negligible. Finally, for the C state, subsequent decay from the A and B states may contribute to the $C \rightarrow X$ fluorescence signal. To investigate this possibility, Corning filters are placed in front of the photomultiplier. The filters eliminate $C \rightarrow X$ fluorescence but allow detection of $A \rightarrow X$ and $B \rightarrow X$ fluorescence. (The $C \rightarrow A$ and $C \rightarrow B$ transitions occur at wavelengths greater than 9000 Å and hence cannot be detected by our photomultiplier.) A cascade contribution is detected, but for the C states of SrX and BaX 1% or less of the integrated fluorescence signal is caused by decay from the intermediate A and B states. The same conclusions are expected to apply to the C states of CaX, namely, cascading effects are much smaller than experimental error.

III. RESULTS

A. Lifetimes

In Fig. 3(a) we show some fluorescence decay traces for the $A\ ^2\Pi_{1/2}$ state of SrBr. The signal-to-noise level of these traces is typical of the majority of the data; however, scans for CaF and SrF states were much noisier because of the lower signal levels. Semilogarithmic plots of fluorescent intensity vs time for the data of Fig. 3(a) are shown in Fig. 3(b). As can be seen, the plots are linear over more than two lifetimes. There was no evidence of systematic curvature in the semilogarithmic plots for any of the 39 electronic states investigated.

Table II summarizes the results of the lifetime measurements on the A, B, and C states of the calcium and strontium monohalides and the C states of the barium monohalides. The columns of the table give, respectively, the laser excitation wavelength, the bandhead nearest to this wavelength, the literature references used to identify the bands, the pressure of the reagent gas used, the number of scans analyzed, the radiative lifetime obtained, and the statistical uncertainty (one standard deviation) in the lifetime measurement. Typically the uncertainty corresponds to errors of 5%–10%; however, for CaF and SrF the error is closer to 20%. As indicated in the experimental section, we expect systematic errors to be less than the statistical uncertainty, i.e., no more than 1 or 2 nsec.

As noted in the Introduction, one of the striking features of the electronic spectra of the alkaline earth monohalides is the close spacing of vibrational sequences and hence the severe overlapping of the rotational envelopes of the bands. This feature virtually precludes excitation of individual v' bands with our laser bandwidth. Nonetheless we have tried, where possible, to excite only low v' levels in order to facilitate a comparison of the excited state lifetimes.

For the $C\ ^2\Pi_{3/2}$ state of BaI the variation of the radiative lifetime with gross changes in v' has been investigated. This is possible because the reactions of CH_3I and CH_2I_2 with Ba populate very different values of v'' (see Table I). (Recall that it is difficult to excite $v'' \rightarrow v' \neq v''$ transition because of the dominance of the $\Delta v = 0$ sequences in the MX spectra.) As can be seen from Table II, no change in lifetime is detectable for $v' = 0$ through $v' = 39$. A variation in lifetime with vibrational state is brought about by changes in the weighted average of the cube of the transition frequency and by the variation of the electronic transition moment with internuclear distance. Because the upper state and lower state potential curves of the MX molecules are so similar, the frequency factor does not vary much with v'.

TABLE II. Measured radiative lifetimes of the calcium, strontium, and barium monohalides.

Molecule	Electronic state[a]	Excitation wavelength (Å)	(v', v'') band[b]	Spectroscopic references used	Pressure (10^{-4} torr)[c]	Number of scans	Lifetime (nsec)	Statistical uncertainty (nsec)[d]
CaF	A_1	6065	(0,0)	e,f	(5)	4	21.9	4.0
	A_2	6037	(0,0)	e,f	(6)	6	18.4	4.1
	B	5309	(0,0)	e,f	(6)	5	25.1	4.0
CaCl	A_1	6209	(2,2)	g	4	7	29.4	1.8
	A_2	6183	(2,2)	g	4	8	28.4	2.6
	B	5934	(0,0)	g	4	9	38.2	3.9
	C_2	3770	(0,0)	g	8	9	25.0	2.1
CaBr	A_1	6276	(1,1)	h	3.5	8	34.2	2.9
	A_2	6252	(1,1)	h	3	10	33.7	1.9
	B	6103	(0,0)	h	5	11	42.9	3.1
	C_1	3952	(0,0)	h	7	10	33.2	4.0
	C_2	3918	(1,1)	h	4	10	31.8	3.7
CaI	A_1	6408	(3,3)	i,j	2	5	41.7	2.3
	A_2	6383	(5,5)	i,j	1.5	5	41.6	3.4
	B	6358	(4,4)	i,j	2.5	9	50.9	1.7
SrF	A_1	6632	(0,0)	k	(3)	4	24.1	2.0
	A_2	6512	(0,0)	k	(3)	4	22.6	4.7
SrCl	A_1	6743	(1,1)	h	2.5	7	31.3	2.7
	A_2	6610	(1,1)	h	2	8	30.4	3.6
	B	6357	(1,1)	h	3	9	38.8	2.1
	C_1	3964	(1,1)	g	2.5	6	26.1	1.9
	C_2	3939	(1,1)	g	3	6	26.0	1.6
SrBr	A_1	6793	(3,3)	h	1.2	7	34.3	2.3
	A_2	6658	(2,2)	h	0.8	8	33.2	1.6
	B	6505	(3,3)	h	1.5	5	42.2	1.6
	C_1	4110	(1,1)	h	2	8	30.3	2.6
	C_2	4056	(1,1)	h	3	6	28.1	1.3
SrI	A_1	6834	(6,5)	l	2.5	6	43.3	1.6
	A_2	6754	(10,10)	l	3	6	41.9	1.3
		6676	(12,11)	l	3.5	10	40.5	3.7
	B	6561	–	m	3	6	46.0	2.0
	C_2	4283	(8,7)	n	4	7	36.0	3.7
BaF	C_1	5001	(0,0)	o	2	11	23.8	2.3
	C_2	4952	(0,0)	o	2	6	23.5	0.7
BaCl	C_1	5245	(0,0)	p	0.4	8	17.5	0.8
	C_2	5140	(0,0)	p	0.9	10	16.6	0.6
BaBr	C_1	5356	(4,4)	h,j	0.7	8	17.9	1.0
	C_2	5198	(8,8)	h,j	0.6	11	16.5	1.4
BaI	C_1	5568[q]	(25,25)	s	3	9	17.9	1.9
	C_2	5383[q]	(0,0)	s	3	8	16.5	1.0
		5348[q]	(21,21)	t	2	7	15.6	1.5
		5320[r]	(39,39)	t	0.7	10	15.9	1.0

[a]For all molecules, A_1, A_2, B, C_1, and C_2 denote, respectively, the $A\,^2\Pi_{1/2}$, $A\,^2\Pi_{3/2}$, $B\,^2\Sigma^+$, $C\,^2\Pi_{1/2}$, and $C\,^2\Pi_{3/2}$ electronic states. It is assumed that in all cases the $^2\Pi$ states are regular, i.e., that the $^2\Pi_{3/2}$ is of higher energy than the $^2\Pi_{1/2}$.

[b]These (v', v'') values are only approximate since bands of the same sequence are badly overlapped. See text.

[c]Pressure of reagent gas in the reaction chamber (uncorrected ionization gauge reading). Figures in parentheses for CaF and SrF show pressures of SF_6 in the chamber during the experiment. However, as noted in the text, the formation of CaF and SrF is not a gas-phase process.

[d]One standard deviation.

[e]A. Harvey, Proc. R. Soc. A 133, 336 (1931).

[f]B. S. Mohanty and K. N. Upadhya, Indian J. Pure Appl. Phys. 5, 523 (1967).

[g]A. E. Parker, Phys. Rev. 47, 349 (1935).

[h]R. E. Harrington, Ph.D. thesis, University of California, Berkeley, CA, 1942.

[i]R. C. Maheshwari, M. M. Shukla, and I. D. Singh, Indian J. Pure Appl. Phys. 9, 327 (1971).

[j]K. Hedfeld, Z. Physik 68, 610 (1931).

[k]M. M. Novikov and L. V. Gurvich, Opt. Spectrosc. 22, 395 (1967).

[l]M. M. Shukla, Indian J. Pure Appl. Phys. 8, 855 (1970).

[m]This work. The spectrum was not resolved. This assignment disagrees with B. R. K. Reddy, Y. P. Reddy, C. G. Rao, and P. T. Rao, Current Sci. (India) 40, 186 (1971), and Ashrafunnisa, D. V. R. Rao, and P. T. Rao, J. Phys. B 6, 1503 (1973).

[n]B. R. K. Reddy, Y. P. Reddy, and P. T. Rao, J. Phys. B 4, 574 (1971).

[o]F. A. Jenkins and A. Harvey, Phys. Rev. 39, 922 (1932).

[p]A. E. Parker, Phys. Rev. 46, 301 (1934).

[q]BaI produced by the reaction Ba + CH_3I. See Table I.

[r]BaI produced by the reaction Ba + CH_2I_2. See Table I.

[s]P. Mesnage, Ann. Phys. (Paris) 11, 5 (1939). The vibrational numbering has been determined by Ref. 2.

[t]Reference 4(a).

TABLE III. Values of $R_e^2(\bar{r})$ (in atomic units) for the calcium, strontium, and barium monohalide band systems calculated from the measured lifetimes. The average of $R_e^2(\bar{r})$ for the $^2\Pi_{1/2}-^2\Sigma^+$ and $^2\Pi_{3/2}-^2\Sigma^+$ subbands is reported. The error limits are obtained from the statistical uncertainties listed in Table II.

	Band system		
Molecule	$A\,^2\Pi-X\,^2\Sigma^+$	$B\,^2\Sigma^+-X\,^2\Sigma^+$	$C\,^2\Pi-X\,^2\Sigma^+$
CaF	5.47±1.1	2.94±0.47	
CaCl	4.07±0.31	2.70±0.28	1.05±0.09
CaBr	3.58±0.25	2.62±0.19	0.93±0.11
CaI	3.10±0.21	2.49±0.08	
SrF	6.01±0.86		
SrCl	4.76±0.49	3.27±0.18	1.17±0.08
SrBr	4.45±0.26	3.22±0.12	1.15±0.08
SrI	3.73±0.20	3.03±0.13	1.08±0.11
BaF			2.58±0.20
BaCl			4.05±0.17
BaBr			4.23±0.30
BaI			4.74±0.44

Thus, the constancy of the radiative lifetime of the BaI $C\ ^2\Pi_{3/2}$ state with v' implies that the square of the electronic transition moment may be treated as a constant of the band system for the vibrational levels studied. We have made this assumption for all the MX band systems investigated.

An examination of Table II reveals that the lifetimes of the CaX and SrX states are remarkably similar but differ from those of BaX. It can also be seen that the lifetimes of the A, B, and C states of CaX and SrX satisfy the inequality,

$$\tau(C) < \tau(A) < \tau(B). \tag{1}$$

Although the lifetimes of the C states of CaF and CaI were not obtained, the A- and B-state lifetimes also satisfy the inequality shown in Eq. (1). This comparison cannot be made for BaX because the lifetimes of only the C states have been measured. It may also be seen from Table II that for CaX and SrX the lifetime of a state increases in going from F to I. Finally we note that within experimental error the lifetimes for the $^2\Pi_{1/2}$ and the $^2\Pi_{3/2}$ fine-structure components of the A and C states are equal for all MX molecules studied.

B. Electronic transition moments

For theoretical computations, the transition moment rather than the lifetime is often the more convenient quantity characterizing the strength of an electronic transition. The radiative lifetime $\tau_{v'}$ of the upper state vibrational level v' of the upper state vibrational level v' is related to the transition probabilities $A_{v'v''}$ by

$$1/\tau_{v'} = \sum_{v''} A_{v'v''}, \tag{2}$$

where the $A_{v'v''}$ are given approximately by[9]

$$A_{v'v''} = \frac{64\pi^4}{3h}\, \nu_{v'v''}^3\, q_{v'v''}\, R_e^2(\bar{r}_{v'v''}). \tag{3}$$

In Eq. (3) $\nu_{v'v''}$, $q_{v'v''}$, and $\bar{r}_{v'v''}$ are, respectively, the transition frequency, Franck–Condon factor, and r centroid of the (v', v'') band, and $R_e^2(r)$ is the square of the electronic transition moment.

Since the electronic spectra of the MX molecules are dominated by the $\Delta v = 0$ sequences, it is a good approximation for the purpose of converting lifetimes to electronic transition moments to set $q_{v'v''} = \delta_{v'v''}$. A more detailed study[2] in the case of the C states of BaX supports this approximation. Note that in general the summation in Eq. (2) is over all electronic states below the state excited. Since 1% or less of the C-state fluorescence arises from decay through intermediate states, we find that the ratio of C-state molecules decaying directly to the X state to those decaying through the A and B states is about 20 or more for the $C\ ^2\Pi$ states of SrX and BaX. In this estimate the fluorescence intensity was corrected for the wavelength response of the photomultiplier. Accordingly, we have ignored the electronic branching in computing the transition moments.[10]

Table III lists the squares of the transition moments calculated from the lifetimes given in Table II, and Fig. 4 illustrates how these vary with halogen atom. It is seen that $R_e^2(\text{A–X}) > R_e^2(\text{B–X}) > R_e^2(\text{C–X})$ for the CaX and SrX molecules. We note that for the A and B states of CaX and SrX the values of $R_e^2(\bar{r})$ decrease in going from F to I. For the C states of CaX and SrX the transition moment appears to be independent of the halogen atom, whereas for the C state of BaX the transition moment increases in going from F to I. We also note that the BaX C states differ from the C states of CaX and SrX in that the magnitude of $R_e^2(\text{C–X})$ for BaX is about 3 times larger.

IV. CALCULATION OF TRANSITION MOMENTS

The ground state calcium, strontium, and barium monohalides (MX) are expected to be well described as ionic molecules (M^+X^-) since the metal ionization potentials I. P. (M) are not much larger than those of the alkali atoms[11] and the electron affinities of the halogen atoms E. A. (X) are known[12] to be large. The purely Coulombic potential, given by $V(r) = \text{I. P. (M)} - \text{E. A. (X)} + e^2/r$, crosses the asymptote of the covalent curve,

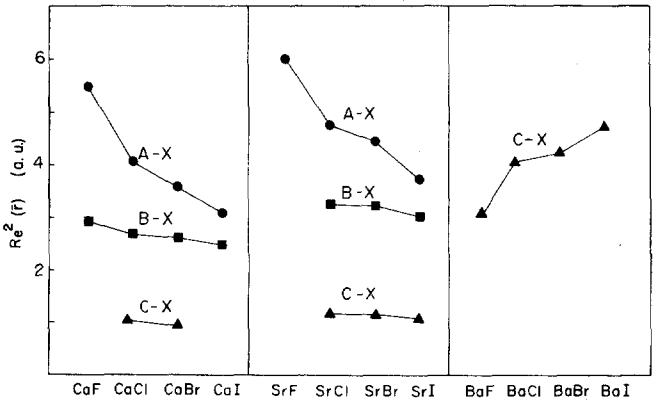

FIG. 4. The electronic transition moments for the $A-X$, $B-X$, and $C-X$ band systems of the calcium, strontium, and barium monohalides.

$V(r)=0$, at internuclear separations, r_c, at least twice that of the equilibrium separation, r_e, with the possible exception of CaI and SrI, for which r_c lies between r_e and $2r_e$. Experimental evidence on the extreme ionicity of the ground state has been provided by Knight, Easley, Weltner, and Wilson[13] through the ESR spectroscopy of MF molecules trapped in inert-gas matrices. They interpret their ^{19}F hyperfine data to mean that less than 4% of the spin density is on the F atom of MgF. For CaF, SrF, and BaF, they find the spin density is even less, as would be expected for these more ionic molecules.

As we have noted in the Introduction, the electronic spectra of the MX molecules appear to be described as "one-electron spectra," in which the electronic transitions correspond to the promotion of an electron in a nonbonding orbital primarily centered on the metal atom to a higher-lying nonbonding orbital also centered on the metal atom. In this simple picture the electronic transitions of the MX molecules can be related to the electronic transitions of the metal atom. What is required then is a means of describing the nonbonding molecular orbital in terms of a truncated set of atomic metal atom wavefunctions.

In the simplest approximation, namely crystal field theory,[14-16] mixing of atomic orbitals is excluded. Here the perturbation by a negative point charge causes an atomic s orbital to become a Σ state, an atomic p orbital to split into a Σ and a Π state with $E(\Pi)<E(\Sigma)$, an atomic d orbital to split into Σ, Π, and Δ states with $E(\Delta)<E(\Pi)<E(\Sigma)$, etc. It seems likely that the $A\ ^2\Pi$ and $B\ ^2\Sigma^+$ states of CaX and SrX are derived from the lowest excited p orbital. On the other hand, the A and B states of BaX have d as well as p character because of the low-lying d state. Accordingly, we will restrict our attention to CaX and SrX in what follows. The crystal field model, in which the $A\ ^2\Pi$ and $B\ ^2\Sigma^+$ states of CaX and SrX are purely $np\pi$ and $np\sigma$, respectively, predicts that the $A-X$ and $B-X$ transition moments are equal.[17] Since this prediction disagrees with our experimental findings, we are led to abandon the crystal field model in favor of a ligand field model,[15,16] in which the wavefunction is a linear superposition of metal orbitals of appropriate symmetry.

The simplest ligand field model is that of a metal ion perturbed by a point charge located at a distance r_e from the metal ion. An attempt has been made to explain the experimental transition moments using this model. The perturbation V of the unpaired electron by the negative point charge is added to the free-ion Hamiltonian. This model was previously invoked by Knight *et al.*[13] in explaining the hyperfine constants of ^{87}SrF and ^{137}BaF. These studies appear to show that the ground $X\ ^2\Sigma^+$ state is well described by the wavefunction,

$$\Psi = c_1|ns\sigma\rangle + c_2|np\sigma\rangle + c_3|(n-1)d\sigma\rangle, \tag{4}$$

with $c_1 \gg c_2$ or c_3.

In the present investigation, Hartree–Fock–Slater (HFS) atomic orbitals[18,19] have been used as the ion basis set since HFS wavefunctions have provided fairly reliable electronic transition probabilities.[20] Computations have been performed only for the calcium compounds. The calculated molecular states are mixtures of a large number of atomic states; however, the $X\ ^2\Sigma^+$ state is still mostly $4s$ in character, as Knight *et al.*[13] found for the three-term expansion in Eq. (4) for SrF and BaF. The large amount of mixing contradicts our intuition that the $A\ ^2\Pi$ and $B\ ^2\Sigma^+$ states are predominantly $4p$ in character. But the more serious objection with this point charge model is that the calculated values of the transition moments vary wildly with internuclear separation. The transition moments from a truncated three-term basis ($4s$, $4p$, $3d$) vary much more smoothly; however, the calculated $A-X$ and $B-X$ transition moments differ from the experimental values by approximately 30% and 60%, respectively. More important, the three-term basis fails to predict the experimental finding that the $A-X$ transition moment is greater than the $B-X$ transition moment. It appears that the point charge model fails when a complete metal ion basis set is used because the perturbation V is too strong and mixes the atomic states too much. The transition moments calculated with the truncated three-term basis set are more reasonable, presumably because some mixing has been prevented by the truncation.

These failures raise the fundamental question whether the use of a metal orbital basis set to represent the ground- and excited-state nonbonding molecular orbitals has any validity. To test this point, we have taken a different approach which nevertheless retains the basic idea that the nonbonding molecular orbital can be described using a truncated metal ion basis set. In this approach, some of the experimental transition moments are used to determine the mixing coefficients and the relevant radial dipole moment integrals. Then these parameters are used to predict other transition moments which can be compared with experimental values. In addition, the radial integrals are compared with those calculated using *ab initio* atomic wavefunctions.

For simplicity, let us assume that the $X\ ^2\Sigma^+$, and $A\ ^2\Pi$, and $B\ ^2\Sigma^+$ states are derived solely from the ns and np states. Thus the molecular states are parameterized by only one empirical constant c,

$$\begin{aligned} |X\ ^2\Sigma^+\rangle &= c\,|ns\sigma\rangle + (1-c^2)^{1/2}|np\sigma\rangle, \\ |B\ ^2\Sigma^+\rangle &= (1-c^2)^{1/2}|ns\sigma\rangle - c\,|np\sigma\rangle, \\ |A\ ^2\Pi\rangle &= |np\pi\rangle. \end{aligned} \tag{5}$$

The $A-X$ and $B-X$ transition moments are then related[17] to the $ns-np$ dipole moment integral

$$R(ns;\ np) = \int_0^\infty r P_{ns}(r) P_{np}(r)\, dr$$

by

$$\begin{aligned} R_e^2(A-X) &= \tfrac{1}{3}c^2 R^2(ns;\ np), \\ R_e^2(B-X) &= \tfrac{1}{3}(2c^2-1)^2 R^2(ns;\ np). \end{aligned} \tag{6}$$

Thus, the value of c may be determined from the ratio of the experimental transition moments, i.e.,

$$c^2 = \tfrac{1}{2} + \tfrac{1}{8}\{Q + [Q(Q+8)]^{1/2}\}, \tag{7}$$

where

$$Q = R_e^2(B-X)/R_e^2(A-X). \tag{8}$$

TABLE IV. Mixing coefficients and radial dipole moment integrals calculated by the empirical two-state model. The error limits reflect the experimental uncertainties in $R_e^2(A-X)$ and $R_e^2(B-X)$. The arbitrary sign of the parameter c has been chosen to be positive.

Molecule	Mixing coefficient c	$\lvert R(ns;\, np)\rvert$ (a.u.)
CaF	0.914 ± 0.033	4.4 ± 0.6
CaCl	0.939 ± 0.020	3.7 ± 0.2
CaBr	0.953 ± 0.018	3.4 ± 0.2
CaI	0.966 ± 0.015	3.2 ± 0.2
SrCl	0.944 ± 0.020	4.0 ± 0.3
SrBr	0.951 ± 0.013	3.8 ± 0.2
SrI	0.967 ± 0.013	3.5 ± 0.2

Using Eqs. (7) and (8), we determine values for the parameter c, as given in Table IV. With these values of c, we are now able to determine the radial integrals $R(ns;\, np)$, using Eq. (6), and the results are also presented in Table IV. Examination of Table IV shows that the degree of mixing of the $ns\sigma$ and $np\sigma$ orbitals in the X and B states is approximately 10% for all the calcium and strontium halides. The values of $R(ns;\, np)$ are almost independent of the halogen atom to within experimental error for a given metal atom. Moreover, the values of $R(ns;\, np)$ are close to the metal ion values obtained from HFS wavefunctions, − 3.73 a.u. for Ca ($n = 4$) and − 4.06 a.u. for Sr ($n = 5$). This agreement provides an indication that use of a metal orbital basis set for the description of the nonbonding molecular orbitals has validity.

The empirically determined mixing coefficient c also permits us to determine the absolute value of the off-diagonal matrix element of the perturbation V, with the assumption that the two diagonal elements of V are equal. Absolute values of the empirically determined $4s-4p$ off-diagonal matrix element range from 0.130 Ry for CaF to 0.067 Ry for CaI, while with the point charge model this element is calculated to be − 0.395 to − 0.199 Ry for values of R from 3.64 to 5.28 a.u. The calculated matrix elements are seen to be a factor of about 3 greater than the empirically determined elements. This provides a further indication that the perturbation V in the point charge model is too large to explain the experimental transition moments.

Finally, it is tempting to extend this empirical model to include the $C-X$ transition moments also. We now allow the $(n-1)\,d$ state to be included. We make the arbitrary assumption that the mixing of the $(n-1)d$ state in the $X\ ^2\Sigma^+$ and $B\ ^2\Sigma^+$ states is zero. This assumption is necessary in order to reduce the number of empirical mixing coefficients to only 2 (parameters c and d),

$$\begin{aligned}
&|X\ ^2\Sigma^+\rangle = c\,|ns\sigma\rangle + (1-c^2)^{1/2}|np\sigma\rangle,\\
&|B\ ^2\Sigma^+\rangle = (1-c^2)^{1/2}|ns\sigma\rangle - c\,|np\sigma\rangle,\\
&|A\ ^2\Pi\rangle = d\,|np\pi\rangle + (1-d^2)^{1/2}|(n-1)d\pi\rangle,\\
&|C\ ^2\Pi\rangle = (1-d^2)^{1/2}|np\pi\rangle - d\,|(n-1)d\pi\rangle.
\end{aligned} \tag{9}$$

The $B-X$ transition moment is the same as in Eq. (6), while the others are

$$\begin{aligned}
R_e^2(A-X) &= \tfrac{1}{3}c^2d^2R^2(ns;\, np) + \tfrac{1}{5}(1-c^2)(1-d^2)R^2(np;\, (n-1)\,d)\\
&\quad + 2cd\left[\tfrac{1}{15}(1-c^2)(1-d^2)\right]^{1/2}R(ns;\, np)\\
&\quad \times R(np;\, (n-1)d),\\
R_e^2(C-X) &= \tfrac{1}{3}c^2(1-d^2)R^2(ns;\, np) + \tfrac{1}{5}(1-c^2)\\
&\quad \times d^2R^2(np;\, (n-1)d) - 2cd\left[\tfrac{1}{15}(1-c^2)(1-d^2)\right]^{1/2}\\
&\quad \times R(ns;\, np)R(np;\, (n-1)d).
\end{aligned} \tag{10}$$

Since there are four unknowns in Eq. (10) but only three experimentally determined quantities, a slightly different approach for the application of the model is taken here. Values for the radial dipole integrals are calculated from HFS metal ion wavefunctions, and the

TABLE V. Mixing coefficients and $C-X$ transition moments (in atomic units) calculated by the empirical three-state model. The error limits reflect the experimental uncertainty in $R_e^2(A-X)$ and $R_e^2(B-X)$ but do not include any uncertainties in the values of $R(ns;\, np)$ and $R[np;\, (n-1)d]$ used.[a]

	Mixing coefficient[c]		$R_e^2(C-X)$	
Molecule[b]	c	d	Calculated	Experimental (Table II)
CaCl	0.939 ± 0.020	+0.997 ± 0.003, −0.949 ± 0.050	0.22 ± 0.20	1.05 ± 0.09
CaBr	0.936 ± 0.020	+0.996 ± 0.004, −0.830 ± 0.045	0.27 ± 0.20	0.93 ± 0.11
CaI	0.931 ± 0.020	+0.939 ± 0.025, −0.768 ± 0.035	1.03 ± 0.25	
SrCl	0.941 ± 0.020	+0.995 ± 0.005, −0.912 ± 0.080	0.28 ± 0.20	1.17 ± 0.08
SrBr	0.940 ± 0.020	+0.988 ± 0.010, −0.860 ± 0.040	0.58 ± 0.25	1.15 ± 0.08
SrI	0.934 ± 0.020	+0.947 ± 0.015, −0.750 ± 0.035	1.25 ± 0.25	1.08 ± 0.11

[a]The values of $R(ns;\, np)$ used are −3.726 (Ca, $n=4$) and −4.509 (Sr, $n=5$), calculated from HFS metal ion wavefunctions using the np configuration to derive the "best" atomic potential according to the variational principle. The values of $R[np;\, (n-1)d]$ used are +2.182 for Ca and +2.742 for Sr, calculated from HFS wavefunctions obtained with the $(n-1)d$ configuration.

[b]CaF is not listed since the calculated mixing coefficient d is imaginary.

[c]The two values of d are both consistent with the experimental $R_e^2(A-X)$ and $R_e^2(B-X)$ values and yield the same calculated value of $R_e^2(C-X)$.

parameter c is calculated from Eq. (6) using the experimental $B-X$ transition moments and the $R(ns; np)$ radial integrals found from the HFS wavefunctions. Then d is obtained from the experimental $A-X$ transition moments, using Eq. (10). It is found that two values of d are consistent with the experimental $R_e^2(A-X)$ and that both yield the same calculated $R_e^2(C-X)$. Values of c, both values of d, and the calculated $R_e^2(C-X)$ are presented in Table V. While there is no way from our limited experimental data to distinguish between the two values of d obtained, it is reasonable to use the values closest to +1 since the $C\ ^2\Pi$ states of CaX and SrX might be expected to be predominantly d in character. The agreement of the calculated and the experimental $C-X$ transition moments is fair (~45% average difference). While the agreement of experimental and calculated $C-X$ transition moments is highly dependent on the values of the radial integrals used, nevertheless the model seems to incorporate the gross features of the X, A, B, and C electronic states for CaX and SrX.

No statement about the BaX $C^2\Pi$ states can be made within the framework of this model since experimental $A-X$ and $B-X$ transition moments are not available. Moreover, since in the Ba ion as well as in the atom the d state lies lower in energy than the p state, our intuition as to the predominant character of the A, B, and C states would need revision. Indeed, the dissimilarity between the BaX transition moments and the CaX and SrX transition moments suggests that the nature of the bonding in the BaX electronic states is quite different.

V. DISCUSSION

To our knowledge, there has been only one previous lifetime study of the alkaline earth monohalides. Capelle, Bradford, and Broida[21] have attempted radiative lifetime measurements using a pulsed dye laser for a number of metal monohalides. However, only for the C states of BaBr and BaCl did they find signals of sufficient intensity to permit a determination. The metal monohalide molecules were produced by reacting metal vapor in an argon carrier gas with Br_2 and Cl_2. Capelle *et al.* report a lifetime of 8 ± 3 nsec for BaBr with 0.07 torr buffer pressure and 22 ± 4 nsec for BaCl at 0.3 torr. The former value differs from our value by a factor of 2, while the latter value agrees with our value to within the combined experimental errors. We are unable to give a definite reason why the agreement for BaBr is not better. However, the effect of systematic errors, such as scattered laser light, collisional quenching, radiation trapping, and the interference from the accompanying chemiluminescence and fluorescence from other species, is not reported. We speculate that their signals are weak because of the large chemiluminescent background since electronically excited MX molecules are produced in the reaction vessel.

The utility of the technique described in this paper for the measurement of radiative lifetimes to 10% accuracy has been demonstrated. For many purposes, such accuracy is quite sufficient. Moreover, this technique is simple to carry out. The use of signal averaging equipment, such as a boxcar integrator, and a careful attention to convolution effects due to the finite width of the laser pulse and the detector response time will allow even more accurate determinations. We note that direct and accurate lifetime measurements have already been performed on atoms using a similar technique.[22]

Ab initio calculations of molecular electronic state lifetimes have not reached a stage of sophistication where they are comparable in accuracy to experimental data in most cases, and for the alkaline earth monohalides studied here reliable calculations may not be available soon. Consequently we have undertaken a semiempirical treatment in the hope that we can elucidate the bonding of the excited states in this homologous series. We have found that the unpaired electron in the MX molecules may be described as being in a nonbonding orbital centered on the metal atom both in the ground and excited states, and this idea has provided a reasonable framework to interpret the experimental transition moments. Moreover, for CaX and SrX the description of the $A\ ^2\Pi$ and $B\ ^2\Sigma^+$ states as predominantly np in character and of the $C\ ^2\Pi$ states as predominantly $(n-1)d$ in character provides a consistent explanation of the magnitudes of the experimental transition moments, while the unpaired electron in BaX has more d character presumably because of the low-lying atomic d orbital. This admittedly crude model does not predict the finer details, such as the variation of the transition moments with halogen atom. Nonetheless, we are able to account for the magnitudes of the CaX and SrX lifetimes to 45% by this model.

ACKNOWLEDGMENTS

We thank W. Weltner, Jr., M. Wilson, and S. Green for useful correspondence and conversations concerning the use of the point charge model. This work was supported in part by the Office of Naval Research under Grant N00014-67-A-0108-0035 and by the Air Force Office of Scientific Research under Grant AFOSR-73-2551.

*Present address: Department of Theoretical Chemistry, Cambridge University, Lensfield Road, Cambridge CB 2 1EW, England.

[1]For a recent compilation of spectroscopic data, see *Spectroscopic Data Relative to Diatomic Molecules*, edited by B. Rosen (Pergamon, Oxford, 1970).

[2]H. W. Cruse, P. J. Dagdigian, and R. N. Zare, Faraday Discuss. Chem. Soc. 55, 277 (1973).

[3]E. D. Stokes, F. B. Dunning, R. F. Stebbings, G. K. Walters, and R. D. Rundel, Opt. Commun. 5, 267 (1972); F. B. Dunning and E. D. Stokes, *ibid.* 6, 160 (1972).

[4](a) H. W. Cruse, P. J. Dagdigian, and R. N. Zare (to be published); (b) unpublished results.

[5]The CaF or SrF fluorescence can be observed with almost undiminished intensity for at least an hour after the chamber has been evacuated.

[6]A. Lurio, Phys. Rev. 136, A376 (1964).

[7]E. Hulpke, E. Paul, and W. Paul, Z. Phys. 177, 257 (1964).

[8]H. Bucka and H. J. Schüssler, Ann. Phys. 7, 225 (1961).

[9]R. W. Nicholls and A. L. Stewart, in *Atomic and Molecular Processes*, edited by D. R. Bates (Academic, New York, 1962), Chap. 2.

[10]From the branching ratios, it is possible to estimate the ratios of electronic transition moments. It is found that the ratio of the $C-X$ moment to the sum of the $C-A$ and $C-B$ mo-

ments is about unity. Thus, the $C-A$ and $C-B$ transitions are as allowed as the $C-X$ transition; the reason why the $C-X$ transition is so much more probable than $C-A$ or $C-B$ is the ν^3 factor in Eq. (3).

[11]C. E. Moore, Circ. U. S. Natl. Bur. Stand. 467 (1949).

[12]For a review of electron affinities, see R. S. Berry, Chem. Rev. 69, 533 (1969).

[13]L. B. Knight, Jr., W. C. Easley, W. Weltner, Jr., and M. Wilson, J. Chem. Phys. 54, 322 (1971).

[14]For a general discussion of crystal field theory, see C. J. Ballhausen, *Introduction to Ligand Field Theory* (McGraw-Hill, New York. 1962).

[15]T. M. Dunn, in *Physical Chemistry: An Advanced Treatise*, edited by H. Eyring, D. Henderson, and W. Yost (Academic, New York, 1970), Vol. 5, Chap. 5.

[16]R. A. Berg and O. Sinanoğlu, J. Chem. Phys. 32, 1082 (1960).

[17]The transition moments between states n and X is defined by $R_e^2(n-X)=\sum_{m=-1}^{+1}|\langle np\Lambda|P(1m)|ns\sigma\rangle|^2$, where $\Lambda=0$ (σ orbital) or 1 (π orbital) for a Σ or Π state, respectively, and $P(1m)$ is the mth component of the dipole moment operator. This may be reduced to $R_e^2(n-X)=(1/3)|\int_0^\infty rP_{ns}(r)\,P_{np}(r)\,dr|^2$, irrespective of whether $\Lambda=0$ or 1. Here $r^{-1}P_{nl}(r)$ is the radial wavefunction of the nlth atomic orbital. For convenience, states of definite parity have not been chosen. If such states are used, the same values for the transition moments are obtained.

[18]J. C. Slater, Phys. Rev. 81, 385 (1951).

[19]The computer programs used are based on those written by F. Herman and S. Skillman, *Atomic Structure Calculations* (Prentice-Hall, Englewood Cliffs, NJ, 1963). The present programs are documented in R. N. Zare, JILA Rept. No. 80 (Joint Institute for Laboratory Astrophysics, Boulder, CO, 1966). See also R. N. Zare, J. Chem. Phys. 45, 1966 (1966).

[20]R. N. Zare, J. Chem. Phys. 47, 3561 (1967). As pointed out in E. Trefftz and R. N. Zare, J. Quant. Spectrosc. Radiat. Transfer 9, 643 (1969), Eqs. (12a) and (12b) should read $a=l'$ if $l'=l''-1$ and $a=-(l''+1)$ if $l'=l''+1$. The rhs of Eq. (11) should be multiplied by -1, and in Eq. (16) the quantity $(-1)p_{\beta\beta'}$ should read $(-1)^{p_{\beta\beta'}}$.

[21]G. A. Capelle, R. S. Bradford, and H. P. Broida, Chem. Phys. Lett. 21, 418 (1973).

[22]T. A. Erdmann, H. Figger, and H. Walther, Opt. Commun. 6, 166 (1972).